

# ***N*-dimensional Vaidya metric with cosmological constant in double-null coordinates**

Alberto Saa\*

*Departamento de Matemática Aplicada,  
IMECC – UNICAMP, C.P. 6065,  
13083-859 Campinas, SP, Brazil.*

A recently proposed approach to the construction of the Vaidya metric in double-null coordinates for generic mass functions is extended to the  $n$ -dimensional ( $n > 2$ ) case and to allow the inclusion of a cosmological constant. Some new exact solutions are presented and some physical examples are explicitly discussed. The results presented here can simplify considerably the study of spherically symmetric gravitational collapse in arbitrary dimensions and also the quasinormal mode analysis of higher dimensional varying mass black-holes.

PACS numbers: 04.50.+h, 04.20.Dw, 04.70.Bw, 04.20.Jb

## **I. INTRODUCTION**

The Vaidya metric[1] is a solution of Einstein's equations with spherical symmetry in the eikonal approximation to a radial flow of unpolarized radiation. For many years, it has been used in the analysis of spherically symmetric collapse and the formation of naked singularities (For references, see the extensive list of [2] and also [3]). It is known that Vaidya metric can be obtained from the Tolman metric, which represents a spherically symmetric dust distribution, by taking appropriate limits in the self-similar case[4]. This result has shed some light on the nature of the so-called shell-focusing singularities[5], as discussed in details in [2, 6, 7, 8]. The Vaidya metric has also proved to be useful in the study of Hawking radiation and the process of black-hole evaporation[9, 10, 11, 12], in the stochastic gravity program[13], and, more recently, in the quasinormal modes analysis of varying mass black holes[14].

The  $n$ -dimensional Vaidya metric is required in many physically relevant situations. The study of the gravitational collapse in higher dimensional spacetimes[15], for instance, has contributed to the elucidation of the formation, nature and eventual visibility of singularities. This last topic belongs to the realm of the celebrated Penrose's Cosmic Censorship Conjecture, see, *e.g.*, [3] for references. Higher dimensional varying mass black holes are also central protagonists in the new phenomenological models with extra dimensions[16]. These objects might be obtained in the LHC at CERN[17] and, once produced, they are expected to decay driven by the emission of Hawking radiation. The analysis of their quasinormal modes can help the understanding of the dynamics of the evaporation process, and could even lead to some observational signs[18].

The inclusion of a cosmological constant  $\Lambda$  in the  $n$ -dimensional Vaidya metric is mainly motivated by the recent intensive activities in the AdS/CFT and dS/CFT

conjectures, see [19] for some references. A cosmological constant is also necessary to allow the discussion of the  $n = 3$  case in the same framework of the higher dimensional cases.

The  $n$ -dimensional Vaidya metric was first discussed in [20]. It can be easily cast in  $n$ -dimensional ( $n > 3$ , the three dimensional case will be discussed latter) radiation coordinates  $(w, r, \theta_1, \dots, \theta_{n-2})$ [15]:

$$ds^2 = - \left( 1 - \frac{2m(v)}{(n-3)r^{n-3}} \right) dv^2 + 2cdrv + r^2 d\Omega_{n-2}^2, \quad (1)$$

where  $c = \pm 1$  and  $d\Omega_{n-2}^2$  stands for the metric of the unity  $(n-2)$ -dimensional sphere, assumed here to be spanned by the angular coordinates  $(\theta_1, \theta_2, \dots, \theta_{n-2})$ ,

$$d\Omega_{n-2}^2 = \sum_{i=1}^{n-2} \left( \prod_{j=1}^{i-1} \sin^2 \theta_j \right) d\theta_i^2. \quad (2)$$

For the case of an ingoing radial flow,  $c = 1$  and  $m(v)$  is a monotone increasing mass function in the advanced time  $v$ , while  $c = -1$  corresponds to an outgoing radial flow, with  $m(v)$  being in this case a monotone decreasing mass function in the retarded time  $v$ . The 4-dimensional Vaidya metric with a cosmological constant in the radiation coordinates has been considered previously in [21].

It is well known that the radiation coordinates are defective at the horizon[22], implying that the Vaidya metric (1) is not geodesically complete in any dimension. (See [23] for considerations about possible analytical extensions). Besides, the cross term  $drdv$  can introduce unnecessary oddities in the hyperbolic equations governing the evolution of physical fields on spacetimes with the metric (1). Typically, the double-null coordinates are far more convenient. This was the main motivation of the Waugh and Lake's work[24], where the problem of casting the 4-dimensional Vaidya metric with  $\Lambda = 0$  in double-null coordinates is considered. As all previous attempts to construct a general transformation from radiation to double-null coordinates have failed, they followed Synge[25] and considered Einstein's equation with spherical symmetry in double-null coordinates *ab initio*. The

---

\*Electronic address: asaa@ime.unicamp.br

resulting equations, however, have revealed to be not analytical solvable for generic mass functions. Waugh and Lake's work was recently revisited in [26], where a semi-analytical approach allowing for generic mass functions was proposed. Such approach has already enhanced considerably the accuracy of the quasinormal modes analysis of 4-dimensional varying mass black holes [14], and it can be also applied to the study of gravitational collapse[26].

Here, we extend the approach proposed in [26] to the  $n$ -dimensional ( $n > 2$ ) case and to allow the inclusion of a cosmological constant  $\Lambda$ . Some new exact solutions are presented. For  $n = 3$ , notably, the non-linearity can be circumvented and the problem can be reduced to the solution of a second order linear ordinary differential equation, opening the possibility for analytical study of large classes of mass functions. We also generalize one of Waugh and Lake's exact solutions, introducing the case corresponding to  $m(v) \propto v^{n-3}$ ,  $n > 3$ , describing a naked or shell focusing singularity in a  $n$ -dimensional spacetime. We present also some explicit examples of the use of the semi-analytical approach to the study of the causal structure of some particular solutions.

In the next Section, the main equations are derived and the exact solutions are presented. Section III is devoted to the introduction of the semi-analytical approach and some examples are presented, particularly the two apparent horizons case of an evaporating black hole in a de Sitter spacetime. The last Section is left to some concluding remarks. This work has two further appendices. The first one presents explicitly the  $n$ -dimensional geometrical quantities necessary to reproduce the equations of the Section II, and the last one contains the polynomial manipulations involved in the calculations of the apparent horizons of Sections II and III.

## II. THE METRIC

The  $n$ -dimensional spherically symmetric line element in double-null coordinates  $(u, v, \theta_1, \dots, \theta_{n-2})$  is given by

$$ds^2 = -2f(u, v)du\,dv + r^2(u, v)d\Omega_{n-2}^2, \quad (3)$$

where  $f(u, v)$  and  $r(u, v)$  are non vanishing smooth functions. We adopt here the same conventions of [24] and [26]. In particular, the indices  ${}_1$  and  ${}_2$  stand for the differentiation with respect to  $u$  and  $v$ , respectively.

The energy-momentum tensor of a unidirectional radial flow of unpolarized radiation in the eikonal approximation is given by

$$T_{ab} = \frac{1}{8\pi}h(u, v)k_a k_b, \quad (4)$$

where  $k_a$  is a radial null vector. We will consider here, without loss of generality, the case of a flow along the  $v$ -direction. The case of simultaneous ingoing and outgoing flows in 4 dimensions was already been considered in [27]. Einstein's equations are less constrained in such

case, allowing the construction of some exact similarity solutions, which, incidentally, can also be generalized to the  $n$ -dimensional case in the light of the present work.

The Einstein's equations with cosmological constant  $\Lambda$

$$R_{ab} - \frac{1}{2}g_{ab}R = -\Lambda g_{ab} + 8\pi T_{ab} \quad (5)$$

implies that, for the for the energy-momentum tensor (4),

$$R = \frac{2n}{n-2}\Lambda. \quad (6)$$

Using (A6) and (6), Einstein's equations for the metric (3) and the energy-momentum tensor (4) read

$$\frac{f_1}{f} - \frac{r_{11}}{r_1} = 0 \quad (7)$$

$$\frac{f_2}{f} - \frac{r_{22}}{r_2} = \frac{h}{n-2} \frac{r}{r_2} \quad (8)$$

$$\frac{f_1 f_2}{f^2} - \frac{f_{12}}{f} - (n-2) \frac{r_{12}}{r} = -\frac{2\Lambda}{n-2}f \quad (9)$$

$$2(rr_{12} + (n-3)r_1 r_2) + (n-3)f = \frac{2\Lambda}{n-2}fr^2 \quad (10)$$

For  $n \neq 3$ , differentiating Eq. (10) with respect to  $u$  and then inserting Eq. (7) leads to

$$\frac{r^{n-2}r_{12}}{f} - \frac{2\Lambda}{(n-2)(n-1)}r^{n-1} = -A, \quad (11)$$

where  $A(v)$  is an arbitrary integration function. The  $n = 3$  case will be considered below. Now, differentiating Eq. (10) with respect to  $v$  and using (8) and (11) gives

$$h = -\left(\frac{n-2}{n-3}\right) \frac{f A_2}{r^{n-2}r_1}. \quad (12)$$

Eq. (7) is ready to be integrated as

$$f = 2Br_1, \quad (13)$$

where  $B(v)$  is another arbitrary integration (and nonvanishing) function. From (12) and (13), one has

$$h = -2\left(\frac{n-2}{n-3}\right) B \frac{A_2}{r^{n-2}}. \quad (14)$$

Finally, by using (10) and (13), Eq. (11) can be written as

$$r_2 = -B \left(1 - \frac{2A}{(n-3)r^{n-3}} - \frac{2\Lambda}{(n-2)(n-1)}r^2\right). \quad (15)$$

Note that (9) follows from Eqs. (13) and (15). Einstein's equations are, therefore, equivalent to the equations (13), (14), and (15), generalizing the results of [24] and [26].

In order to interpret physically the arbitrary integration functions  $A(v)$  and  $B(v)$ , let us transform from the double-null coordinates back to the radiation coordinates

by means of the change  $(u, v) \rightarrow (r(u, v), v)$ . Such transformation casts (3) in the form

$$ds^2 = 4Br_2dv^2 - 4Bdrdv + r^2d\Omega_{n-2}^2, \quad (16)$$

where (13) were used. Comparing (1) and (16) and taking into account (15), it is clear that with the choice

$$B = -\frac{1}{2} \frac{A_2}{|A_2|}, \quad (17)$$

for  $A_2 \neq 0$ , the function  $A(v)$  should represent the mass of the  $n$ -dimensional solution, suggesting the following  $n$ -dimensional generalization of the mass definition for  $\Lambda = 0$  based in the angular components of the Riemann tensor[28]:

$$m = \frac{n-3}{2} r^{n-3} R_{\theta_1 \theta_k \theta_1}^{\theta_k}, \quad (18)$$

$k > 1$ , see (A5) and (15). Note that for constant  $A$ , the choice of the function  $B(v)$  is irrelevant since it can be absorbed by a redefinition of  $v$ . Note also that the weak energy condition applied for (4) requires, from (14), that  $BA_2 \leq 0$ . Since  $B$  must be nonvanishing from (13),  $A(v)$  must be a monotone function.

The Kretschmann scalar  $K = R_{abcd}R^{abcd}$  could be also invoked to interpret the function  $A$ . Taking into account Eqs. (13) and (15), we have from (A8)

$$K = 4 \frac{(n-1)(n-2)^2}{(n-3)} \frac{A^2}{r^{2(n-1)}} + \frac{8n}{(n-1)(n-2)^2} \Lambda^2. \quad (19)$$

It is clear from (19) that  $r = 0$  is a singularity for  $A \neq 0$ .

The problem now may be stated in the following way: given the mass function  $A(v)$  and the constant  $B$ , Eq. (15) shall be integrated and  $r(u, v)$  is obtained. Then,  $f(u, v)$  and  $h(u, v)$  are calculated from (13) and (14). The arbitrary function of  $u$  appearing in the integration of (15) must be chosen properly in order to have a non-vanishing  $f(u, v)$  function from (13)[24]. Unfortunately, this procedure is not analytically solvable in general. Waugh and Lake, nevertheless, were able to find some regular solutions for Eqs. (13)-(15) for  $n = 4$  and  $\Lambda = 0$ , namely the linear ( $A(v) = \lambda cv$ ) and a certain exponential ( $A(v) = \frac{1}{\beta}(\alpha \exp(\beta cv/2) + 1)$ ) mass functions ( $\lambda, \alpha$ , and  $\beta$  are positive constants,  $c = \pm 1$ , corresponding to ingoing/outgoing flow, respectively). The 4-dimensional linear mass case was also considered in [8] in great detail and in a more general situation (the case of a charged radial null fluid). In [26], another 4-dimensional exact solution corresponding to  $A(v) = \kappa/v$  and  $\Lambda = 0$  was also presented and discussed. These are the only varying mass analytical solutions obtained in double-null coordinates so far. We notice, however, that Kuroda was able to construct a transformation from radiation to double-null coordinates for some other particular mass functions in four dimensions[10].

In the following, we will present a semi-analytical procedure to attack the problem of solving Eqs. (13)-(15)

for general mass functions obeying the weak energy condition, generalizing in this way the results of [26] obtained for  $n = 4$  and  $\Lambda = 0$ . The approach allows us to construct qualitatively conformal diagrams, identifying horizons and singularities, and also to evaluate specific geometric quantities. Before, however, we notice that the Waugh and Lake's linear 4-dimensional solution can be also generalized for  $n$ -dimensions. Let us consider the mass function

$$A(v) = \lambda v^{n-3}, \quad (20)$$

$v \geq 0$ ,  $\lambda > 0$ . For this mass function and  $\Lambda = 0$ , with the choice (17), Eq. (15) reads

$$r_2 = \frac{1}{2} - \frac{\lambda}{n-3} \left( \frac{v}{r} \right)^{n-3}, \quad (21)$$

which can be integrated as

$$\ln v + \int^{(r/v)} \left( s - \frac{1}{2} + \frac{\lambda}{n-3} s^{-(n-3)} \right)^{-1} ds = D(u), \quad (22)$$

where  $D(u)$  is an arbitrary integration function, implying, from Eq. (13), that

$$f = -\frac{v^{n-2} D_1}{r^{n-3}} \left[ \left( \frac{r}{v} \right)^{n-2} - \frac{1}{2} \left( \frac{r}{v} \right)^{n-3} + \frac{\lambda}{n-3} \right]. \quad (23)$$

The integration function  $D$  must be chosen in order to have a regular  $f$ . As in the 4-dimensional case originally considered by Waugh and Lake, we have three qualitatively distinct cases. For instance, with  $\lambda > \lambda_n^c$ , where

$$\lambda_n^c = \left( \frac{n-3}{2(n-2)} \right)^{n-2}, \quad (24)$$

the quantity inside the square brackets in (23) does not vanish, see the Appendix B. The integral in (22) can be (numerically) evaluated and, for instance with the Waugh and Lake's choice  $D(u) = -u$ ,  $r(u, v)$  can be also (numerically) determined. The resulting causal structures are the same of the Waugh and Lake's 4-dimensional case. In the next section, we will construct the relevant conformal diagrams for the three qualitatively distinct cases as an application of the semi-analytical approach. The other cases correspond to  $\lambda = \lambda_n^c$  and  $0 < \lambda < \lambda_n^c$ .

### A. The three dimensional case

In lower dimensional ( $n < 4$ ) spacetimes, the Riemann tensor is completely determined by its traces, namely the Ricci tensor and the scalar curvature, implying some qualitative distinct behavior for the solutions of Einstein's equations in these situations[29]. For  $n = 3$ , Eq. (10) reads

$$\frac{rr_{12}}{f} + \Lambda r^2 = 0. \quad (25)$$

It is interesting to compare this last equation with (11). Eq. (13) is still valid, and using it, Eq. (25) can be integrated leading to

$$r_2 + \Lambda Br^2 = C, \quad (26)$$

where  $C$  is an arbitrary integration function which we call, by convenience,  $C(v) = -B(v)A(v)$ , leading to

$$r_2 = -B(-A - \Lambda r^2), \quad (27)$$

which corresponds to the 3-dimensional counterpart of Eq. (15). Eq. (9) for  $n = 3$  also follows from (13) and (27). As for the  $n$ -dimensional case, by using (13) and (27), one gets from (8) the last equation

$$h = -B \frac{A_2}{r}. \quad (28)$$

One can show that the integration functions  $A$  and  $B$  have the same physical interpretation of the higher dimensional cases. For instance, by introducing the radiation coordinates we have for the 3-dimensional case

$$ds^2 = -(2B)^2 (-A - \Lambda r^2) dv^2 - 4B dr dv + r^2 d\theta^2. \quad (29)$$

It is clear that with the choice (17) for  $B$ , the function  $A$  plays the role of the BTZ black-hole mass[30] ( $\Lambda < 0$  in this case). Note, however, that for  $n = 3$  there is no purely angular components of the Riemann tensor and, therefore, there is no equivalent of the mass definition (18). The Kretschmann scalar in this case is

$$K = 12\Lambda^2. \quad (30)$$

In contrast with the  $n$ -dimensional case, the non-linearity present in (27) can be easily circumvented. Let us consider  $A_2 > 0$ ,  $B = -1/2$ , and  $\Lambda = -1/\ell^2$  (Other cases follow straightforwardly). By introducing the linear second order ordinary differential equation

$$w''(v) - \frac{A(v)}{4\ell^2} w(v) = 0, \quad (31)$$

it is easy to show that

$$r(u, v) = -2\ell^2 \frac{P(u)w_a'(v) + w_b'(v)}{P(u)w_a(v) + w_b(v)}, \quad (32)$$

is solution of (27), where  $w_a(v)$  and  $w_b(v)$  are the two linearly independent solutions of (31), and  $P(u)$  is an arbitrary function. The second order linear equation (31) has analytical solution in closed form for many functions  $A(v)$ . For instance, with  $A(v) \propto v^\alpha$  (or  $A(v) \propto \exp \alpha v$ ),  $\alpha \in \mathbb{R}$ , Eq. (31) is equivalent to the Bessel equation, after an appropriate redefinition of  $v$ . Even for the case where no solution in closed form can be obtained, the main analytical properties of  $w(v)$  can be inferred from (31) due to its linearity.

### III. SEMI-ANALYTICAL APPROACH

Equations (13), (14), and (15) (or (27) and (28) for the 3-dimensional case) can be attacked by the same semi-analytical procedure presented in [26]. Eqs. (15) and (27) along  $u$  constant are first order ordinary differential equations in  $v$ . One can evaluate the function  $r(u, v)$  in any point by solving the  $v$ -initial value problem knowing  $r(u, 0)$ . For instance, the usual constant curvature empty spacetimes ( $A = 0$ ) can be obtained by choosing  $r(u, 0) = u/2$ , leading to

$$\int_{r_0}^r \left(1 - \frac{2\Lambda}{(n-2)(n-1)} s^2\right)^{-1} ds = \frac{1}{2}(v+u). \quad (33)$$

As it is expected, for the  $n$ -dimensional de Sitter case ( $\Lambda > 0$ ),  $r = \sqrt{(n-2)(n-1)/2\Lambda}$  corresponds to a cosmological horizon.

For  $n > 3$ , the curves  $r(v)$  given by

$$-\frac{2\Lambda}{(n-2)(n-1)} r^{n-1} + r^{n-3} = \frac{2A(v)}{n-3} \quad (34)$$

correspond (if they indeed exist) to the frontiers of certain regions of the  $(v, r)$  plane where the solutions of (15) have qualitative distinct behaviors. For the de Sitter case, (34) defines two non intersecting curves, whereas for the anti de Sitter case ( $\Lambda < 0$ ) there is only one curve. (See Appendix B). Let us suppose, for instance, a de Sitter case with  $A_2(v) > 0$  (and  $B = -1/2$ . Outgoing radiation flows, 3-dimensional spacetimes, or the anti de Sitter case follow in a straightforward manner).

Let us call  $r_{EH}(v)$  and  $r_{CH}(v)$  the solutions of (34), see Fig. 1. Due to (15), for all points of the plane  $(v, r)$  below  $r_{EH}(v)$ ,  $r_2 < 0$ . Hence, any solution entering in this region will, unavoidably, reach the singularity at  $r = 0$ , with finite  $v$ . Suppose a given solution  $r_i(v)$  with initial condition  $r_i(0) = r_i$  enters into this region. As the uniqueness of solutions for (15) is guaranteed for any point with  $r > 0$ , solutions never cross each other in the plane  $(v, r)$  for  $r > 0$ . Any solution starting at  $r(0) < r_i$  is confined the the region below  $r_i(v)$ , and it will also reach the singularity at  $r = 0$  with finite  $v$ . On the other hand, suppose that a given solution  $r_e(v)$  with initial condition  $r_e(0) = r_e$  never enters into region bellow the curve  $r_{EH}(v)$ . Any solution starting at  $r(0) > r_e$  is, therefore, confined to the region above  $r_e(v)$  and will escape from the singularity. Keeping in mind that these solutions correspond to null trajectories with  $u$  constant, it is possible to infer the causal structure of the spacetime from their qualitative behavior and an appropriate choice for the initial conditions  $r(u, 0)$ . The curve  $r_{EH}(v)$ , for instance, plays the role of an apparent event horizon. For a given  $v$ , all solutions in Fig. 1 such that  $r(v) \leq r_{EH}(v)$  will be captured by the singularity. Solutions for which  $r(v) > r_{EH}(v)$  are temporally free, but they may find themselves trapped later if  $r_{EH}(v)$  increases. The event horizon will correspond to the last of these solutions trapped by the singularity.

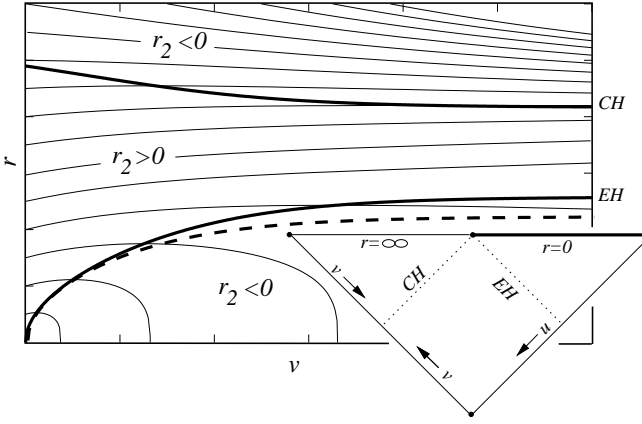


FIG. 1: In the region below the function  $r_{EH}(v)$  (the apparent event horizon), all solutions have  $r_2 < 0$ . Any solution that enters into this region will reach the singularity at  $r = 0$  with finite  $v$ . Solutions confined to the  $r_2 > 0$  region always escape from the singularity and tend asymptotically to  $r_{CH}(v)$  (the apparent cosmological horizon). The region above  $r_{CH}(v)$  corresponds to the cosmological exterior, any solution there also tends asymptotically to  $r_{CH}(v)$ . The dashed line would correspond to the apparent event horizon for the case of a vanishing  $\Lambda$  (The unique solution of (34) for  $\Lambda = 0$ ). The conformal diagram is inserted. (The case depicted here corresponds to:  $n = 5$ ,  $\Lambda = 1$ , and  $A(v) = (6/5) \tanh v$ ,  $v \geq 0$ .)

In the region between  $r_{EH}(v)$  and  $r_{CH}(v)$ , the solutions of (15) have  $r_2 > 0$ . They escape from  $r_{EH}(v)$  and tend asymptotically to  $r_{CH}(v)$ , which plays the role of an apparent cosmological horizon. The region above  $r_{CH}(v)$  corresponds to the cosmological exterior (See, for instance, [31]. For  $A = 0$ , the cosmological exterior region corresponds to the choice  $r_0 = \infty$  in (33)). There,  $r_2 < 0$  and the solutions also tend asymptotically to  $r_{CH}(v)$ . The case where  $r_{EH}(v)$  and  $r_{CH}(v)$  converge to the same function gives rise to  $n$ -dimensional Nariai solution[32].

For more details on the approach, see [26]. Let us present now some applications.

### A. Waugh and Lake generalized solutions

As the first application of the semi-analytical approach, let us consider the generalized Waugh and Lake solutions corresponding to the choice (20) for the mass function,  $n > 3$ , and  $\Lambda = 0$ . From the discussion of Section II, we expect three qualitatively distinct case according to the value of  $\lambda$ . In fact, these solutions have the same causal structure for all  $n > 3$ . The frontier of the region in the  $(v, r)$  plane where all the solutions of (21) reach the singularity at  $r = 0$  corresponds to the straight line

$$r_0(v) = \left( \frac{2\lambda}{n-3} \right)^{\frac{1}{n-3}} v. \quad (35)$$

Taking the  $v$ -derivative of (21), one gets

$$r_{22} = \lambda \frac{v^{n-2}}{r^{n-3}} \left( -1 + \frac{1}{2} \frac{v}{r} - \frac{\lambda}{n-3} \left( \frac{v}{r} \right)^{n-3} \right). \quad (36)$$

The regions in the plane  $(v, r)$  where the solutions obeys  $r'' = 0$  are the straight lines corresponding to the solutions of

$$\left( \frac{r}{v} \right)^{n-2} - \frac{1}{2} \left( \frac{r}{v} \right)^{n-3} + \frac{\lambda}{n-3} = 0 \quad (37)$$

One can now repeat the analysis done for the  $n = 4$  case by considering the three qualitative different cases according to the value of  $\lambda$  and the possible solutions of (37). For this purpose, we will consider the solutions of (21) with the initial condition  $r(u, 0) \propto u$ .

For  $\lambda > \lambda_n^c$ , with  $\lambda_n^c$  given by (24), Eq. (37) has no solution and  $r'' < 0$  for all points with  $v > 0$ . The only relevant frontier in the plane  $(v, r)$  is the  $r_0(v)$  straight line. All solutions of (21) are concave functions and cross the  $r_2 = 0$  line, reaching the singularity with a finite  $v$  which increases monotonically with  $u$ . The causal structure of the corresponding spacetime is very simple. There is no horizon, and the future cone of all points ends in the singularity at  $r = 0$ . The associated conformal diagram is depicted in Fig. 2.

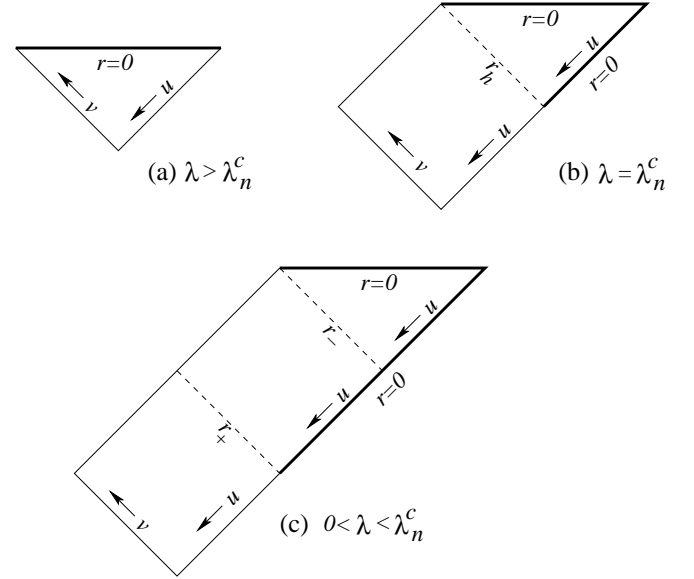


FIG. 2: Conformal diagrams corresponding to the mass function (20). Cases (b) and (c) exhibit naked and shell focusing singularities. For all cases, the curves in the  $(v, r)$  are similar to those ones presented in [26], corresponding to the  $n = 4$  case.

For  $\lambda = \lambda_n^c$ ,  $r_{22} = 0$  only on the line

$$r_h(v) = \frac{n-3}{2(n-2)} v. \quad (38)$$

This straight line itself is a solution of (21). All other solutions are concave functions. Note that  $r_h(v) > r_0(v)$

for  $v > 0$ . We have two distinct qualitative behavior for the null trajectories along  $u$  constant. All solutions starting at  $r(0) > 0$  are confined to the region above  $r_h(v)$ . They never reach the singularity, all trajectories reach  $\mathcal{I}^+$ . However, in the region below  $r_h(v)$ , we have infinitely many concave trajectories starting and ending in the (shell-focusing) singularity. They start at  $r(0) = 0$ , increase in the region between  $r_h(v)$  and  $r_0(v)$ , cross the last line and reach unavoidably  $r = 0$  again, with finite  $v$ . The trajectory  $r_h(v)$  plays the role of an event horizon, separating two regions with distinct qualitative behavior: one where constant  $u$  null trajectories reach  $\mathcal{I}^+$  and another where they start and end in the singularity. This behavior is only possible, of course, because the solutions of (21) fail to be unique at  $r = 0$ . The relevant conformal diagram is also shown in Fig. 2.

For  $0 < \lambda < \lambda_n^c$ , we have three distinct regions according to the concavity of the solutions. They are limited by the two straight lines  $r_-(v)$  and  $r_+(v)$  corresponding to the solutions of (37). We have  $r_0(v) < r_-(v) < r_+(v)$  for  $v > 0$ . Both straight lines  $r_-(v)$  and  $r_+(v)$  are also solutions of (21). Between them, solutions are convex. Above  $r_+$  and below  $r_-$ , solutions are concave. The last line is the inner horizon. Inside, the null trajectories with constant  $u$  start and end in the singularity  $r = 0$ . The line  $r_+$  is an outer horizon. Between them, the constant  $u$  null trajectories starts in the naked singularity and reach  $\mathcal{I}^+$ . Beyond the outer horizon, all constant  $u$  null trajectories escape the singularity, see Fig. (2).

## B. Black-hole evaporation in a de Sitter spacetime

As an example of using the semi-analytical approach for  $\Lambda \neq 0$ , let us consider the case of a evaporating black hole due to Hawking radiation in a de Sitter  $n$ -dimensional ( $n > 3$ ) spacetime. The mass decreasing rate for these  $n$ -dimensional black holes can be obtained from the  $n$ -dimensional Stefan-Boltzmann law (see, for instance, [33]), leading to

$$\frac{dm}{dt} = -am^{-2/(n-3)} \quad (39)$$

where  $a > 0$  is the effective  $n$ -dimensional Stefan-Boltzmann constant. Eq. (39) can be immediately integrated, leading to

$$m(t) = m_0 \left(1 - \frac{t}{t_0}\right)^{\frac{n-3}{n-1}}, \quad (40)$$

where  $t_0$  in the lifetime of a black hole with initial mass  $m_0$ ,

$$a \frac{n-1}{n-3} t_0 = m_0^{(n-1)/(n-3)}. \quad (41)$$

We recall that (39) is not expected to be valid in the very final stages of the black hole evaporation, where the

appearance of new emission channels for Hawking radiation can induce changes in the value of the constant  $a$ [34], and maybe even the usual adiabatic derivation of Hawking radiations is no longer valid. We do not address these points here. We assume that the black hole evaporates completely obeying (40) for all  $0 \leq t \leq t_0$ .

We can consider now a  $n$ -dimensional Vaidya metric with a mass term of the form given by (40). This is the first case of an outgoing radial flux we consider, and according to (17),  $B = 1/2$ . However, in this case,  $f(u, v)$  has different sign and the temporal directions for the  $B = -1/2$  case are now spacelike. The transformation  $(u, v) \rightarrow (v, -u)$  restores the temporal and spatial directions[26]. One needs to keep in mind that, for  $B < 0$  (ingoing radiation fields),  $v$  corresponds to the advanced time, whereas for  $B > 0$  (outgoing radiation fields),  $u$  should correspond to the retarded time. In this case, the equivalent of Eq. (15) for a mass function as (40) reads

$$r_1 = \frac{1}{2} \left( 1 - \frac{2m_0}{n-3} \frac{(1-u/t_0)^{\frac{n-3}{n-1}}}{r^{n-3}} - \frac{2\Lambda}{(n-1)(n-2)} r^2 \right), \quad (42)$$

$u \geq 0$ . We can now apply the same procedure we have used. We call  $r_{EH}(u)$  and  $r_{CH}(u)$  the curves on the  $(u, v)$  plane delimiting the regions where the solutions of (42) have qualitatively distinct behavior. (See Fig. 3). In

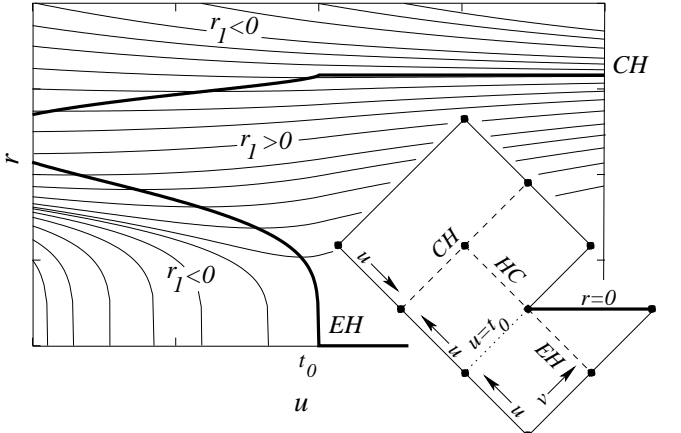


FIG. 3: The  $(u, v)$  plane for an evaporating black hole in a  $n$ -dimensional de Sitter spacetime. The apparent horizons  $r_{EH}(u)$  and  $r_{CH}(u)$  delimit the regions where the solutions of (42) have qualitatively distinct behavior. Since the black hole vanishes for  $u = t_0$ , for  $u > t_0$  the only remaining horizon corresponds to  $r_{CH}(u)$ . The conformal diagram is inserted. For  $u < t_0$ , it represents an usual black hole. For  $u > t_0$ , we have the empty space left after the vanishing of the black hole. The dashed line  $HC$  (extension of the black hole horizon  $EH$ ) is a Cauchy horizon. Beyond it, we have a breakdown of predictability due to the naked singularity left by the black hole. The cosmological exterior region (the region above  $CH$ ) is completely insensitive to the singularity. (The case depicted here corresponds to:  $n = 6$ ,  $\Lambda = 5/2$ , and  $m_0 = t_0 = 1$ ,  $u \geq 0$ .)

this case, since  $A_1 < 0$ , the curve  $r_{EH}(v)$  decreases and

reach  $r = 0$  for  $u = t_0$ , corresponding to the total vanishing of the black hole. After this point,  $r_{CH}(v)$  is the only horizon (a cosmological one) of this spacetime. Before  $u = t_0$ , however, some solutions of (42) that crossed  $r_{EH}(v)$  could reach the singularity at  $r = 0$ . The exterior cosmological region (region of the  $(u, r)$  plane above  $r_{CH}(v)$ ) is insensitive to the singularity. The resulting conformal diagram shown in Fig. 3. It represents a spacetime with a cosmological horizon and, in its interior, a black hole that evaporates completely leaving behind a naked singularity.

#### IV. CONCLUSION

We considered here the problem of constructing the  $n$ -dimensional Vaidya metric with a cosmological constant  $\Lambda$  in double-null coordinates, generalizing the work [26], where a semi-analytical approach is proposed to attack the equations derived first by Waugh and Lake[24] for  $n = 4$  and  $\Lambda = 0$ . Some new exact solutions are also presented. For  $n = 3$ , in particular, the problem reduces to the solution of the second order linear ordinary differential equation (31), allowing the analytical study of large classes of mass functions  $A(v)$ . As an example, for  $\Lambda < 0$  and  $A(v) = m_0 + m_1 \tanh v$ ,  $m_0 > m_1$ , Eq. (31) is equivalent to the hypergeometric equation, after a proper redefinition of  $v$ . This situation corresponds to a BTZ black hole with mass  $m_0 - m_1$  that accretes some mass smoothly and ends with mass  $m_0 + m_1$ . This kind of exact solution, with two “asymptotic BTZ” regions ( $v \rightarrow \pm\infty$ ) is very interesting to the study of creation of particles in non stationary spacetimes[35].

The generalized semi-analytical approach is also useful to the study of quasinormal modes of varying mass  $n$ -dimensional black holes. In particular, an interesting point is the study of the stationary regime for quasinormal modes, described in [14], in higher dimensional space and in the presence of a cosmological constant. The semi-analytical approach can help the understanding of the relation anticipated by Konoplya[36] for the quasinormal modes of  $n$ -dimensional black holes with  $\Lambda = 0$ :  $\omega_R \propto nr_0^{-1}$ , where  $\omega_R$  and  $r_0$  stand for the oscillation frequency and the black hole radius, respectively. Some preliminary results[18] suggests the existence of a stationary regime such that, for slowly varying mass  $n$ -dimensional black holes,  $\omega_R(v) \propto nr_0^{-1}(v)$ . As an application for  $\Lambda \neq 0$ , we have the dynamical formation of a Nariai solution, which could be accomplished by choosing  $A(v)$  such that  $r_{EH}(v) \rightarrow r_{CH}(v)$  for large  $v$ . These points are still under investigation.

#### Acknowledgments

This work was supported by FAPESP and CNPq.

#### APPENDIX A: SOME GEOMETRICAL QUANTITIES

We present here some geometrical quantities necessary to reproduce the equations of Section II. Such quantities are the  $n$ -dimensional ( $n > 2$ ) generalization of the 4-dimensional ones calculated previously by Synge[25] and Waugh and Lake[24]. Only nonvanishing terms are given.

Recall that our  $n$ -dimensional line element is given by

$$ds^2 = -2f(u, v)du dv + r^2(u, v)d\Omega_{n-2}^2, \quad (A1)$$

where  $d\Omega_{n-2}^2$  is the unity  $(n-2)$  sphere, assumed here to be spanned by the angular coordinates  $\theta_i$ ,  $i = 1 \dots (n-2)$ ,

$$d\Omega_{n-2}^2 = \sum_{i=1}^{n-2} \left( \prod_{j=1}^{i-1} \sin^2 \theta_j \right) d\theta_i^2. \quad (A2)$$

The Christoffel symbols are

$$\begin{aligned} \Gamma_{uu}^u &= \frac{f_1}{f}, & \Gamma_{vv}^v &= \frac{f_2}{f}, \\ \Gamma_{u\theta_k}^{\theta_k} &= \frac{r_1}{r}, & \Gamma_{v\theta_k}^{\theta_k} &= \frac{r_2}{r} \\ \Gamma_{\theta_k\theta_k}^u &= r \left( \prod_{i=1}^{k-1} \sin^2 \theta_i \right) \frac{r_2}{f} \\ \Gamma_{\theta_k\theta_k}^v &= r \left( \prod_{i=1}^{k-1} \sin^2 \theta_i \right) \frac{r_1}{f} \\ \Gamma_{\theta_k\theta_k}^{\theta_j} &= -\frac{1}{2} \left( \prod_{i=j+1}^{k-1} \sin^2 \theta_i \right) \sin 2\theta_j, \quad (k > j) \\ \Gamma_{\theta_k\theta_k}^{\theta_k} &= \cot \theta_j, \quad (k \neq j) \end{aligned} \quad (A3)$$

The totally covariant Riemann tensor  $R_{abcd}$  is given by

$$\begin{aligned} R_{uvuv} &= \frac{f_1 f_2}{f} - f_{12}, \\ R_{u\theta_k u\theta_k} &= r \left( \prod_{i=1}^{k-1} \sin^2 \theta_i \right) \left( \frac{f_1 r_1}{f} - r_{11} \right) \\ R_{v\theta_k v\theta_k} &= r \left( \prod_{i=1}^{k-1} \sin^2 \theta_i \right) \left( \frac{f_2 r_2}{f} - r_{22} \right), \\ R_{u\theta_k \theta_k v} &= r \left( \prod_{i=1}^{k-1} \sin^2 \theta_i \right) r_{12} \\ R_{\theta_k \theta_k \theta_j \theta_k} &= r^2 \left( \prod_{l=1}^{j-1} \sin^2 \theta_l \right) \left( \prod_{i=j+1}^{k-1} \sin^2 \theta_i \right) \\ &\quad \times \left( 1 + 2 \frac{r_1 r_2}{f} \right), \quad (k > j). \end{aligned} \quad (A4)$$

Using (13), we get from the purely angular components of the Riemann tensor:

$$R_{\theta_1 \theta_k \theta_1}^{\theta_k} = 1 + \frac{r_2}{f}, \quad (A5)$$

for any  $k > 1$ . As for the  $n = 4$  case[28], such components are invariant under transformations involving solely the double-null coordinates  $(u, v) \rightarrow (U(u, v), V(u, v))$  and are candidates for defining the mass of the solution for  $\Lambda = 0$ .

The Ricci tensor, obtained by the contraction  $R_{ab} = R_{cab}{}^c$  is given by

$$\begin{aligned} R_{uu} &= (n-2) \left( \frac{f_1 r_1}{fr} - \frac{r_{11}}{r} \right) \\ R_{uv} &= \frac{f_1 f_2}{f^2} - \frac{f_{12}}{f} - (n-2) \frac{r_{12}}{r} \\ R_{vv} &= (n-2) \left( \frac{f_2 r_2}{fr} - \frac{r_{22}}{r} \right) \end{aligned} \quad (\text{A6})$$

$$R_{\theta_k \theta_k} = \left( \prod_{i=1}^{k-1} \sin^2 \theta_i \right) \left[ \frac{2}{f} (rr_{12} + (n-3)r_1 r_2) + (n-3) \right]$$

Two scalar quantities are relevant for our purposes: the scalar curvature  $R = g^{ab} R_{ab}$  and the Kretschmann scalar  $K = R_{abcd} R^{abcd}$ . They are given by

$$\begin{aligned} R &= \frac{2}{f} \left( f_{12} - \frac{f_1 f_2}{f} \right) \\ &\quad + \frac{n-2}{r^2} \left( 4 \frac{r_1 r_2}{f} + (n-3) \left( 1 + \frac{rr_{12}}{f} \right) \right), \end{aligned} \quad (\text{A7})$$

and

$$\begin{aligned} K &= 2 \frac{(n-1)(n-3)}{r^2} \left[ \frac{4}{f^2} \left( r_{12}^2 + r_{11} r_{22} + \frac{r_1 r_2 f_1 f_2}{f^2} - \frac{r_{22} r_1 f_1}{f} - \frac{r_{11} r_2 f_2}{f} \right) + \frac{1}{r^2} \left( 1 + 4 \frac{r_1^2 r_2^2}{f^2} + \frac{r_1 r_2}{f} \right) \right] \\ &\quad + \frac{4}{f^2} \left( \frac{f_1^2 f_2^2}{f^2} + f_{12}^2 - 2 \frac{f_{12} f_1 f_2}{f} \right). \end{aligned} \quad (\text{A8})$$

## APPENDIX B: SOME POLYNOMIAL RESULTS

The evaluation of the zeros of  $f$  given by (23) involves finding the positive roots of the polynomial

$$p_n(x) = x^{n-3} \left( x - \frac{1}{2} \right) = -\frac{\lambda}{n-3}, \quad (\text{B1})$$

for  $\lambda > 0$  and  $n > 3$ . The only roots of  $p_n(x)$  are  $x = 1/2$  and  $x = 0$ , the latter with multiplicity  $n-3$ . For positive  $x$ ,  $p_n(x) < 0$  only in the interval  $x \in (0, 1/2)$ . The minimal value of  $p_n(x)$  in such an interval corresponds to

$$p_n(x_{\max}^p) = -\frac{1}{n-3} \lambda_n^c = -\frac{1}{n-3} \left( \frac{n-3}{2(n-2)} \right)^{n-2}, \quad (\text{B2})$$

where

$$x_{\max}^p = \frac{n-3}{2(n-2)}, \quad (\text{B3})$$

the unique root of  $p'_n(x)$  in the interval. Thus, for  $\lambda > \lambda_n^c$ , the polynomial (B1) has no roots. For  $\lambda = \lambda_n^c$  there is only one root ( $x = x_{\max}^p$ ), while for  $0 < \lambda < \lambda_n^c$ , there are two roots  $x_1$  and  $x_2$ , with  $0 < x_1 < x_{\max}^p < x_2 < 1/2$ .

The determination of the curves (34) involves the evaluation of the positive roots of the polynomial

$$q_n(x) = x^{n-3} \left( 1 - \frac{2\Lambda}{(n-1)(n-2)} x^2 \right) = \frac{2A}{n-3}, \quad (\text{B4})$$

with  $A > 0$  and  $n > 3$ . For the anti de Sitter case,  $\Lambda < 0$ , the only root of  $q_n(x)$  is  $x = 0$ ,  $q_n(x)$  and  $q'_n(x)$  are both

positive for all  $x > 0$ , and, therefore, (B4) has only one positive root. Equation (34), in this case, defines only one curve.

On the other hand, for the de Sitter case,  $\Lambda > 0$ ,  $q_n(x)$  has always 3 roots:  $x = \pm \sqrt{(n-1)(n-2)/2\Lambda}$  and  $x = 0$ , the last with multiplicity  $n-3$ . Moreover, for positive  $x$ ,  $q_n(x) \geq 0$  only for  $x \in [0, \sqrt{(n-1)(n-2)/2\Lambda}]$ , and the maximum value of  $q_n(x)$  in such an interval is  $q_n(x_{\max}^q)$ , where

$$x_{\max}^q = \sqrt{\frac{(n-2)(n-3)}{2\Lambda}}, \quad (\text{B5})$$

the only point of the interval where  $q'_n(x) = 0$ . For  $0 < 2A/(n-3) < q_n(x_{\max}^q)$ , (B4) has always two roots  $x_1$  and  $x_2$ ,  $x_1 < x_{\max}^q < x_2$ . For  $2A/(n-3) = q_n(x_{\max}^q)$ , there is only one root  $x = x_{\max}^q$ , and for  $2A/(n-3) > q_n(x_{\max}^q)$  there is no root at all. In this case, provided that  $0 < 2A/(n-3) < q_n(x_{\max}^q)$ , Eq. (34) defines two curves  $r_{EH}(v)$  and  $r_{CH}(v)$  (See Fig. 1), such that  $r_{EH}(v) < x_{\max}^q < r_{CH}(v)$ .

If  $r(v)$  is a curve given by (34), its derivative is given by

$$r'(v) = \frac{2}{n-3} \frac{A'(v)}{r^{n-4}} \left( (n-3) - \frac{2\Lambda}{n-2} r^2 \right)^{-1}. \quad (\text{B6})$$

If  $\Lambda < 0$ , it is clear that  $r'(v)$  has the same sign of  $A'(v)$ . For  $\Lambda > 0$ , the curves  $r_{EH}(v)$  and  $r_{CH}(v)$  have qualitatively distinct behavior. Since  $r_{EH}(v) < x_{\max}^q$ ,  $r'_{EH}(v)$  has the same sign of  $A'(v)$ . The curve  $r_{CH}(v)$  has the converse behavior, since  $r_{CH}(v) > x_{\max}^q$ .

---

[1] H. Stephani *et al.*, *Exact Solutions of Einstein's Field Equations*, Cambridge University Press, second edition, 2002.

[2] K. Lake, Phys. Rev. Lett. **68**, 3129 (1992).

[3] P.S. Joshi, *Global Aspects in Gravitation and Cosmology*, Oxford University Press, 1993.

[4] J.P.S. Lemos, Phys. Rev. Lett. **68**, 1447 (1992); C. Hellaby, Phys. Rev. **D49**, 6484 (1994).

[5] D.M. Eardley and L. Smarr, Phys. Rev. **D19**, 2239 (1979).

[6] Y. Kuroda, Progr. Theor. Phys. **72**, 63 (1984).

[7] K. Lake and T. Zannias, Phys. Rev. **D41**, 3866 (1990).

[8] K. Lake and T. Zannias, Phys. Rev. **D43**, 1798 (1991).

[9] W.A. Hiscock, Phys. Rev. **D23**, 2813 (1981).

[10] Y. Kuroda, Progr. Theor. Phys. **71**, 100 (1984); *ibid.*, 1422 (1984).

[11] W. Biernacki, Phys. Rev. **D41**, 1356 (1990).

[12] R. Parentani, Phys. Rev. **D63**, 041503(R) (2001).

[13] B.-L. Hu and E. Verdaguer, Living Rev. Relativity **7**, 3 (2004).

[14] E. Abdalla, C.B.M.H. Chirenti, and A. Saa, Phys. Rev. **D74**, 084029 (2006).

[15] S.G. Ghosh and N. Dadhich, Phys. Rev. **D64**, 047501 (2001); *ibid.*, **D65**, 127502 (2002).

[16] N. Arkani-Hamed, S. Dimopoulos and G. Dvali, Phys. Lett. **429B**, 263 (1998); Phys. Rev. **D59**, 086004 (1999); I. Antoniadis, N. Arkani-Hamed, S. Dimopoulos and G. Dvali, Phys. Lett. **436B**, 257 (1998).

[17] S. Dimopoulos and G. Landsberg, Phys. Rev. Lett. **87**, 161602 (2001). For reviews, see: M. Cavaglia, Int. J. Mod. Phys. **A18**, 1854 (2003); P. Kanti, Int. J. Mod. Phys. **A19**, 4899 (2004).

[18] E. Abdalla, C.B.M.H. Chirenti, and A. Saa, *Quasinormal modes for evaporating mini black holes*, to appear.

[19] S. Nojiri and S.D. Odintsov, JHEP **0112**, 033 (2001); S. Nojiri, S.D. Odintsov, and S. Ogushi, Phys. Rev. **D65**, 023521 (2002); Int. J. Mod. Phys. **A17**, 4809 (2002); B. McInnes, Nucl. Phys. **B627**, 311 (2002).

[20] B.R. Iyer and C.V. Vishveshwara, Pramana **32**, 749 (1989).

[21] A. Patino and H. Rago, Phys. Lett. **121A**, 329 (1987).

[22] R. Lindquist, R. Schwartz, and C. Misner, Phys. Rev. **137**, 1364 (1965).

[23] F. Fayos, M.M. Martin-Prats, and J.M.M. Senovilla, Class. Quantum Grav. **12** 2565 (1993).

[24] B. Waugh and K. Lake, Phys. Rev. **D34**, 2978 (1986).

[25] J. Synge, Ann. Mat. Pura. Appl. **98**, 239 (1974).

[26] F. Girotto and A. Saa, Phys. Rev. **D70**, 084014 (2004).

[27] P.R. Holvorcem, P.S. Letelier, and A. Wang, J. Math. Phys. **36**, 3663 (1995).

[28] C. Hernandez and C. Misner, Astrophys. J. **143**, 452 (1966); M.E. Cahil and G.C. McVittie, J. Math. Phys. **11**, 1382 (1970); *ibid.*, 1392 (1970).

[29] J.D. Brown, *Lower dimensional gravity*, World Scientific, 1988.

[30] M. Banados, C. Teitelboim and J. Zanelli, Phys. Rev. Lett. **69**, 1849 (1992).

[31] B. Carter, in *Black Holes*, edited by C. DeWitt and B.S. DeWitt, Gordon and Breach, 1973.

[32] V. Cardoso, O.J.C. Dias, and J.P.S. Lemos, Phys. Rev. **D70**, 024002 (2004).

[33] M. Cavaglia, S. Das, and R. Maartens, Class. Quantum Grav. **15**, L205 (2003).

[34] D.N. Page, Phys. Rev. **D13**, 198 (1976); 3260 (1976).

[35] C. W. Bernard and A. Duncan, Annals Phys. **107**, 201 (1977).

[36] R.A. Konoplya, Phys. Rev. **D68**, 024018 (2003).